Chalcogenide Letters Vol. 22, No. 1, January 2025, p. 23 - 31

# Influence of neodymium doping on radiation shielding properties of yttrium lead borotellurite glass system

M. R. S. Nasuha [a,*], H. Azhan [b,c], L. Hasnimulyati [c], W. A. W. Razali [c], Y. Norihan [c]

[a] *Faculty of Applied Sciences, Universiti Teknologi MARA, Perak Branch, Tapah Campus, 35400 Tapah Road, Perak, Malaysia*

[b] *Faculty of Plantation and Agrotechnology, Universiti Teknologi MARA, Melaka Branch, Jasin Campus, 77300 Merlimau, Melaka, Malaysia*

[c] *Faculty of Applied Sciences, Universiti Teknologi MARA, Pahang Branch, Jengka Campus, 26400 Bandar Tun Abdul Razak Jengka, Pahang, Malaysia*

The need for effective shielding materials has grown as radiation-based technologies have been more widely used. Glasses doped with rare earth elements like neodymium oxide, are promising candidates due to their enhanced radiation attenuation properties. Using Phy-X software, this research examines how neodymium oxide doping affects the shielding properties of yttrium lead borotellurite glass. X-ray diffraction confirmed the amorphous structure, while density measurements showed increased density with neodymium oxide addition. The Phy-X software calculated radiation shielding parameters for gamma energies from $10^{-3}$ to $10^{5}$ MeV. The results demonstrate that neodymium oxide improves gamma irradiation attenuation and enhances the glass system's radiation shielding capabilities.

(Received October 2, 2024; Accepted January 7, 2025)

*Keywords:* Neodymium, Yttrium, Lead borotellurite, Radiation shielding

## 1. Introduction

Radiation refers to the emission and propagation of energy in the form of particles or waves across space or a medium. It is categories into two types which are ionizing and non-ionizing radiation. Alpha, beta, gamma, electron, proton, neutron, and x-rays are examples of radiation that is frequently used in medical, science, industry, agriculture, as well as nuclear power plants. However, exposure to extremely high doses of radiation, such as proximity to an atomic blast, can cause severe health effects, including acute radiation syndrome and skin burns. It may also lead to long-term health issues like cardiovascular diseases and cancer [1, 2]. Therefore, radiation shielding was required to block the radiation from entering the body and destroying biological materials like DNA and tissue [3].

With the increasing utilization of radiation-based technologies, there is a pressing need for innovative materials capable of efficiently attenuating radiation while remaining lightweight, cost-effective, and environmentally friendly [4]. Therefore, to develop suitable shielding materials, it is crucial to comprehend the interaction between radiation and matter, as well as the gamma energy absorption and attenuation in materials. Other than that, various parameters influence the effectiveness of shielding materials, including mass attenuation coefficient (MAC), linear attenuation coefficient (LAC), mean free path (MFP), half value layer (HVL), effective atomic number ($Z_{eff}$), and effective electron density ($N_{eff}$) [5]. Materials with exceptional optical transparency and strong radiation attenuation characteristics, such as optical glasses, are good options for radiation shielding [6]. A high level of shielding capability and resistance against radiation are combined in an excellent shielding glass to provide complete protection for those who are working in potentially hazardous environments [7, 8].

* Corresponding author: nasuharafien@uitm.edu.my
https://doi.org/10.15251/CL.2025.221.23

Rare earth element doped glass materials have become attractive options for radiation shielding due to their ability to offer tailored properties suitable for radiation attenuation [9]. Among these rare earth dopants, neodymium ion has attracted considerable attention owing to its high emission cross-section, broad optical absorption range as well as high quantum efficiency [10, 11]. Lead borotellurite glass system, characterized by the presence of lead oxide (PbO), boron oxide ($B_2O_3$), as well as tellurium oxide ($TeO_2$), has been extensively studied for its versatile properties, including high density, good chemical durability, wide optical transmission range and simultaneously create glass that is highly stable [12]. However, to explore the reliance of radiation shielding behavior, incorporating rare earth dopants such as neodymium oxide into this glass matrix presents an opportunity to enhance its radiation shielding capabilities while maintaining desirable glass properties.

Consequently, the purpose of this study is to use the Phy-X program to examine the theoretical radiation shielding characteristics of neodymium doping on lead borotellurite glasses. A direct link to the web-based program Phy-X immediately accessible via https://phy-x.net/module/physics/shielding/ [13] It is essential to comprehend how the concentration of neodymium affects the effectiveness of radiation shielding for optimizing the composition of these glasses for practical applications in radiation shielding.

## 2. Materials and method

To analyze the radiation shielding capability of a sample material, the radiation shielding parameter for different concentration of neodymium doped yttrium lead borotellurite glass have been analyzed by using the Phy-X software [13]. A step-by-step guide is necessary for the user to achieve the desired results. First, the composition was entered on the Phy-X main page to define the glass using the "+" symbol to separate the oxides. In Phy-X, the formula for the glass sample was input as listed in Table 1. Next, the glass density was provided at this stage and energy range of $10^{-3}$ to $10^5$ MeV was selected. The data of MAC, LAC, MFP, HVL, $Z_{eff}$, and $N_{eff}$ were then chosen and saved in an Excel file for further analysis, discussion, and interpretation. The details of glass composition with varying $Nd_2O_3$ concentration from 0.0 to 2.5 mol% and density of all the samples used in this present study was calculated from an earlier work done by M.R.S. Nasuha et al., (2021) as listed in Table 1 [14].

*Table 1. $Nd_2O_3$ amounts, Sample compositions and Density of the glass sample.*

| $Nd_2O_3$ (mol%) | Glass Composition | Density (g/cm$^3$) |
|---|---|---|
| 0.0 | $0.490H_3BO_3$-$0.35TeO_2$-$0.15PbO$-$0.01Y_2O_3$-$0Nd_2O_3$ | 4.591 |
| 0.5 | $0.485H_3BO_3$-$0.35TeO_2$-$0.15PbO$-$0.01Y_2O_3$-$0.005Nd_2O_3$ | 4.783 |
| 1.0 | $0.480H_3BO_3$-$0.35TeO_2$-$0.15PbO$-$0.01Y_2O_3$-$0.01Nd_2O_3$ | 4.870 |
| 1.5 | $0.475H_3BO_3$-$0.35TeO_2$-$0.15PbO$-$0.01Y_2O_3$-$0.015Nd_2O_3$ | 4.920 |
| 2.0 | $0.470H_3BO_3$-$0.35TeO_2$-$0.15PbO$-$0.01Y_2O_3$-$0.02Nd_2O_3$ | 5.203 |
| 2.5 | $0.465H_3BO_3$-$0.35TeO_2$-$0.15PbO$-$0.01Y_2O_3$-$0.025Nd_2O_3$ | 5.286 |

Source: M.R.S. Nasuha et al., (2021) [14]

## 3. Results and discussions

Data on the MAC shows an increasing trend as the amount of $Nd_2O_3$ increases from 0.001 MeV to 100000 MeV of photon energy except at 1 MeV (Table 2). The increment of MAC is related to glass density as it shows a similar trend with increase in concentration of $Nd_2O_3$ from 0 mol% to 2.5 mol% (Table 1). This found that when the concentration of $Nd_2O_3$ increases, the possibility of photon attenuation is rises as well [4]. Therefore, this finding suggested that the $Nd_2O_3$ dopant in the glass samples is suitable to be used in shielding gamma radiation as gamma ray photons in generally have energy larger than 0.1 MeV [15]. At 1 MeV of photon energy, the MAC reduce can pertaining to the substitution of a higher atomic number of Nd (Z = 60) for a lower atomic number of B (Z = 5) [16].

*Table 2. MAC of $Nd_2O_3$ doped yttrium lead borotellurite glass.*

| Energy (MeV) | Mass Attenuation Coefficient (MAC) | | | | | |
|---|---|---|---|---|---|---|
| | 0.0% $Nd_2O_3$ | 0.5% $Nd_2O_3$ | 1.0% $Nd_2O_3$ | 1.5% $Nd_2O_3$ | 2.0% $Nd_2O_3$ | 2.5% $Nd_2O_3$ |
| 0.001 | 5943.230 | 5954.025 | 5964.583 | 5974.910 | 5985.0150 | 5994.904 |
| 0.01 | 91.209 | 92.884 | 94.521 | 96.123 | 97.690 | 99.224 |
| 0.1 | 2.145 | 2.153 | 2.160 | 2.167 | 2.174 | 2.181 |
| 1 | 0.06347 | 0.06343 | 0.06340 | 0.06336 | 0.06333 | 0.06329 |
| 10 | 0.03493 | 0.03503 | 0.03514 | 0.03524 | 0.03533 | 0.03543 |
| 100 | 0.05556 | 0.05584 | 0.05611 | 0.05638 | 0.05664 | 0.05690 |
| 1000 | 0.06813 | 0.06848 | 0.06883 | 0.06916 | 0.06949 | 0.06982 |
| 10000 | 0.07085 | 0.07122 | 0.07158 | 0.07193 | 0.07228 | 0.07261 |
| 100000 | 0.07128 | 0.07165 | 0.07201 | 0.07236 | 0.07271 | 0.07305 |

The MAC values depended not only on the density and composition of $Nd_2O_3$ in the glass but also depend on the incident photon energy [17]. The MAC values versus photon energy for the sample was plotted in Fig. 1 respectively. For this analysis, a broad range of low, medium as well as high energy levels of photon were used. Therefore, we are able to comprehend the glass samples' attenuation performance across a variety of energies. It was observed that in Fig. 1, the MAC decline quickly as the photon energy increases at range from 0.001 MeV to 0.004 MeV. This showed that at lower photon energy, more photons are being attenuated. This result might be related to the photoelectric effect interaction between gamma ray photons and the glass sample's atoms [16]. A sharp rise in the same photon energy area is seen, which is related to the gamma photons being absorbed by the Neodymium element's K-shell electrons [18]. Within the spectrum of medium energy of 0.004 Mev to 0.02 MeV, the MAC steadily drop with the enhancement of photon energy. The MAC steadily decline is attribute to the dominance of Compton scattering interaction [19]. At energy range higher than 0.02 MeV, the MAC values almost constant as a result of the pair production become the dominant. Similar graph pattern is also displayed for glass samples with varying composition such as the glass system compose of $TeO_2$–$MgO$–$Na_2O$–$Nd_2O_3$ [18]

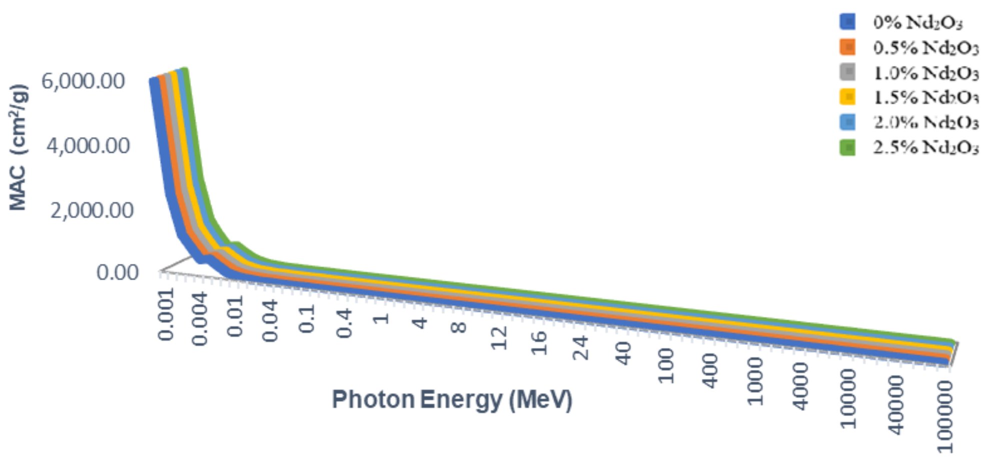


*Fig. 1. MAC of glass samples with different $Nd_2O_3$ concentrations against energy.*

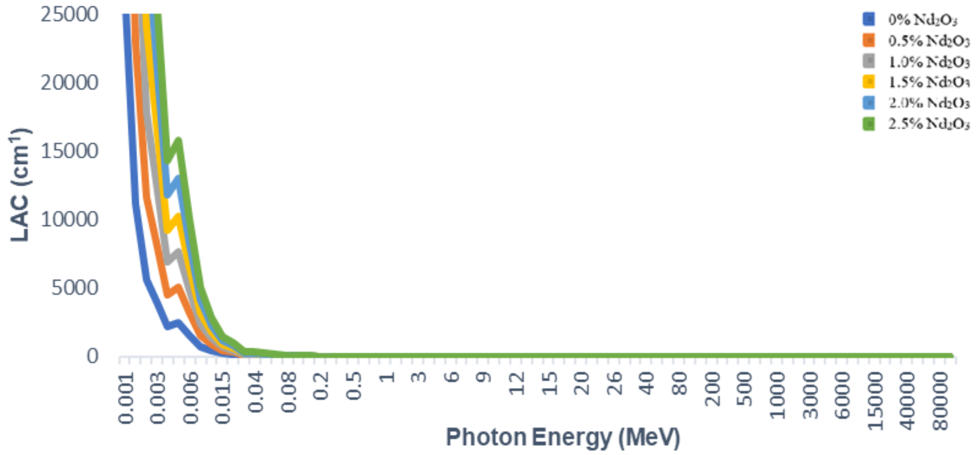


*Fig. 2. LAC of glass samples with different $Nd_2O_3$ concentrations against energy.*

Fig. 2 presents the LAC against photon energy for the glass samples. The pattern of the graph is similar for all the glass sample but each of them changes by a factor according to the density of the glass. According to Fig. 2, the glass sample containing 0 mol% of $Nd_2O_3$ has the lowest LAC and the LAC gradually increases as the concentration of $Nd_2O_3$ increases. So, 2.5 mol% of $Nd_2O_3$ has the best shielding potential since it has highest LAC due to its high density compared to the other glass samples.

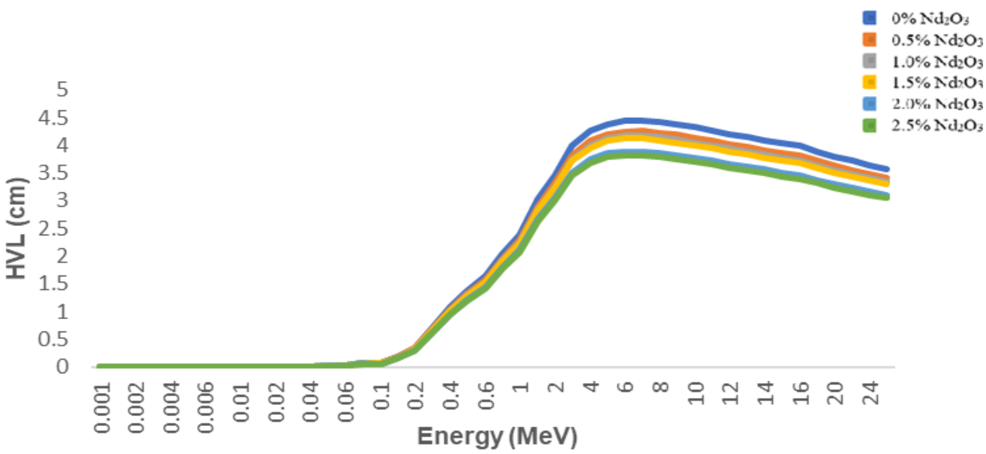


*Fig. 3. HVL of glass samples with different $Nd_2O_3$ concentrations against energy.*

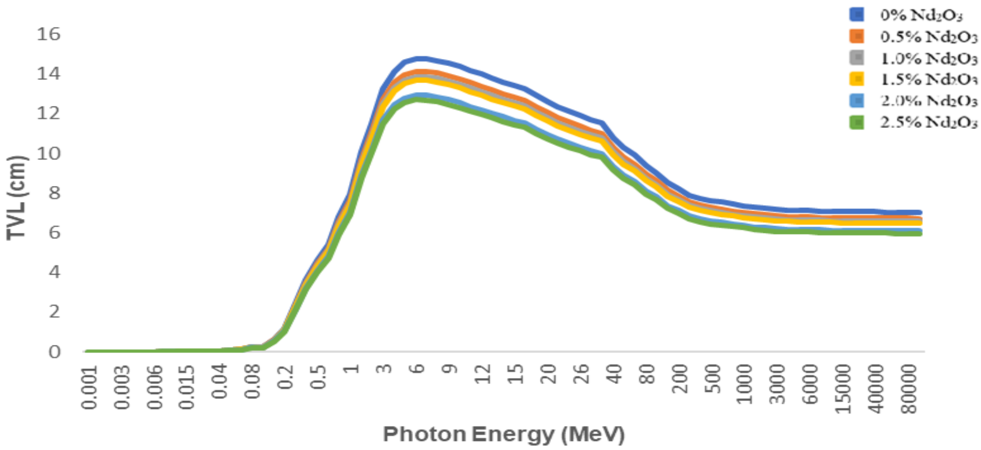


*Fig. 4. TVL of glass samples with different $Nd_2O_3$ concentrations against energy.*

In designing any radiation shielding material, the HVL and TVL are two important factors that need to be considered because they show how thick an absorber has to be in order to reduce radiation intensity to half and a tenth of its starting value, respectively [20]. The smaller values of HVL and TVL present a good gamma ray protection capability [21]. The HVL and TVL data were calculated directly from Phy-X software. The data obtained were analysed in the form of graphs as plotted in Fig. 3 and Fig. 4. As shown in the figures, the values of HVL and TVL are almost zero at lower energy level in range 0.001 to 0.04 MeV. Then, at energy range between 0.008 to 6.0 MeV the values start to increase rapidly before its start to decrease and remains constant at energy level higher than 6.0 MeV. Additionally, we observed that the HVL and TVL values are decreases as the concentration of $Nd_2O_3$ increases from 0.5 to 2.5 mol%. This effect is likely due to the increasing percentage of $Nd_2O_3$ in the glass sample. As $Nd_2O_3$ content rises from 0 to 2.5 mol%, the glass density increases. As a result, the increase in density lead to a reduction in the HVL and TVL values. Therefore, based on both graphs, the glass sample with 2.5 mol% of $Nd_2O_3$ has the lowest HVL and TVL values, making it the most optimal gamma ray protection capability.

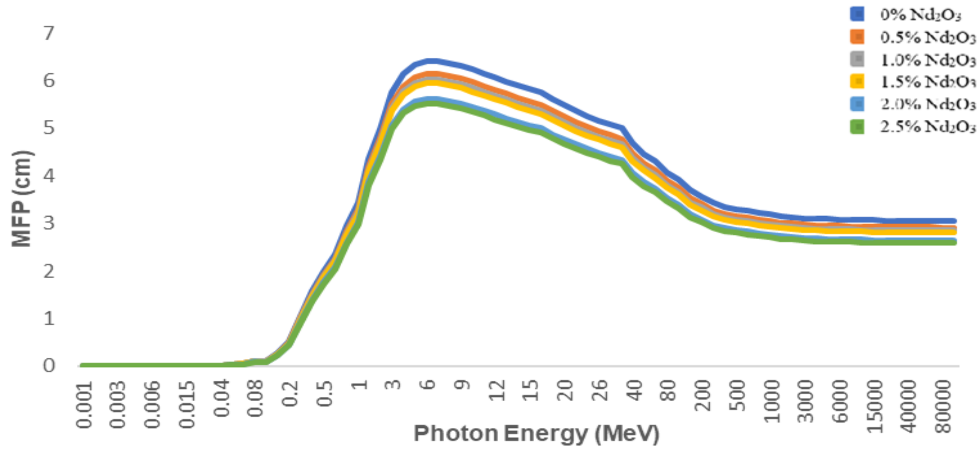


*Fig. 5. MFP of glass samples with different $Nd_2O_3$ concentrations against energy.*

Fig. 5 shows the variation in MFP against photon energy for glass samples with different $Nd_2O_3$ concentrations. The MFP, which represents the average distance that photons travel before interacting with the material [22]. From the graph, the MFP values decrease with increasing $Nd_2O_3$ concentration across all photon energies, particularly noticeable at higher energy levels. At lower photon energies below 0.1 MeV, all samples exhibit similar MFP values, indicating negligible differences in photon absorption. However, as the photon energy increases between 0.1 to 10 MeV, a significant reduction in MFP occurs, with the sample containing 2.5 mol% $Nd_2O_3$ showing the lowest MFP values across most energy levels. This suggests that increasing $Nd_2O_3$ content enhances the photon absorption capability of the glass, as the density of the glass increases with higher $Nd_2O_3$ concentrations. Consequently, the higher-density glasses with more $Nd_2O_3$ reduce photon penetration more effectively, resulting in lower MFP values [23]. The trend in MFP values, particularly the reduction observed as $Nd_2O_3$ concentration increases, supports the observation that glass samples with higher $Nd_2O_3$ content offer improved shielding properties against radiation. This behaviour aligns with previous studies that have shown an inverse relationship between glass density and MFP [24].

Another important consideration when evaluating a material's capacity to attenuate gamma radiation is its effective atomic number ($Z_{eff}$). Prior research has demonstrated that materials with a high $Z_{eff}$ exhibit excellent radiation shielding properties [25]. The $Z_{eff}$ values were plotted as a function of photon energy (MeV) for investigated glass samples with various concentrations of $Nd_2O_3$ as shown in Fig. 6. The $Z_{eff}$ values increase in the energy region below than 10 keV and then decrease as the energy increase to 1 MeV. In the same photon energy region, there is a sharp rise in $Z_{eff}$ peaking around 0.02 MeV. This is indicative of the photoelectric effect is strongly influenced by the atomic number as well as suggests that the inclusion of $Nd_2O_3$ with its high atomic number, significantly impacts photon interactions in this region [26]. The peak is more pronounced at higher $Nd_2O_3$ concentrations, reflecting the strong atomic number dependence of the photoelectric effect. As the photon energy increases, photon-matter interactions are dominated by processes like Compton scattering and pair production, which are less sensitive to the variations of atomic number [6]. Therefore, the data suggest that the sample with 2.5 mol% of $Nd_2O_3$ concentrations is more effective at lower photon energies, making them suitable for applications requiring enhanced photon attenuation, such as radiation shielding in medical and nuclear fields [27]. This trend of data is aligned with previous study that have been done by A. Acikgoz et al., (2023) [18].

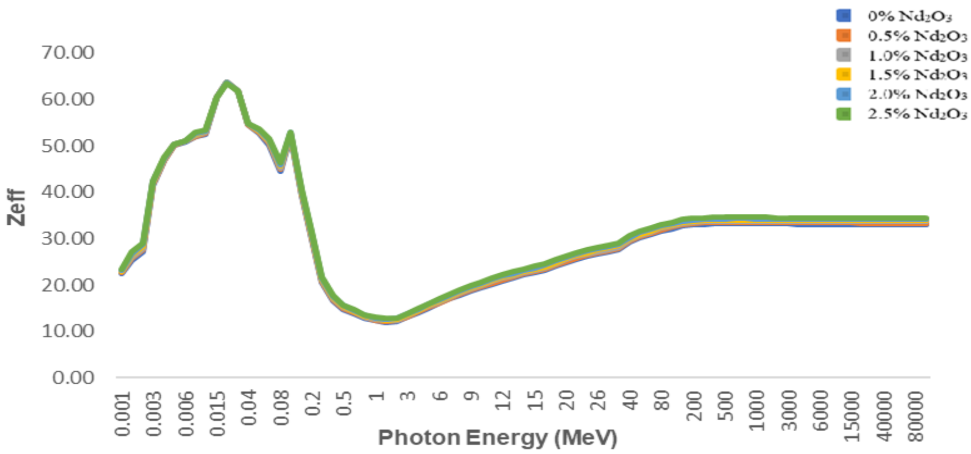


*Fig. 6. $Z_{eff}$ of glass samples with different $Nd_2O_3$ concentrations against energy.*

The values of $N_{eff}$ versus photon energy are show in **Fig. 7**. Since the graph follows a pattern similar to the $Z_{eff}$ parameter, a comparable approach can be explained. In the low energy region lower than 0.1 MeV, the $Z_{eff}$ and $N_{eff}$ show the same graph pattern and both obtain highest value attributed to the photoelectric absorption. Above intermediate region, the parameters gradually decline with increase in the photon energy due to Compton scattering prevails. Then, they become constant in the greater photon energy level starting around 100 MeV due to the dominance of pair production. A equivalent trend in the graphs of $Z_{eff}$ and $N_{eff}$ for photon energies ranging from 1 keV to 100 GeV was also noted by H.O. Tekin *et al*., (2021) and Y. Elmahroug *et al*., (2015) [16, 19]. The $Z_{eff}$ and $N_{eff}$ values were thought to be affected by the chemical composition, as well as the molecular and thermal environment [28].

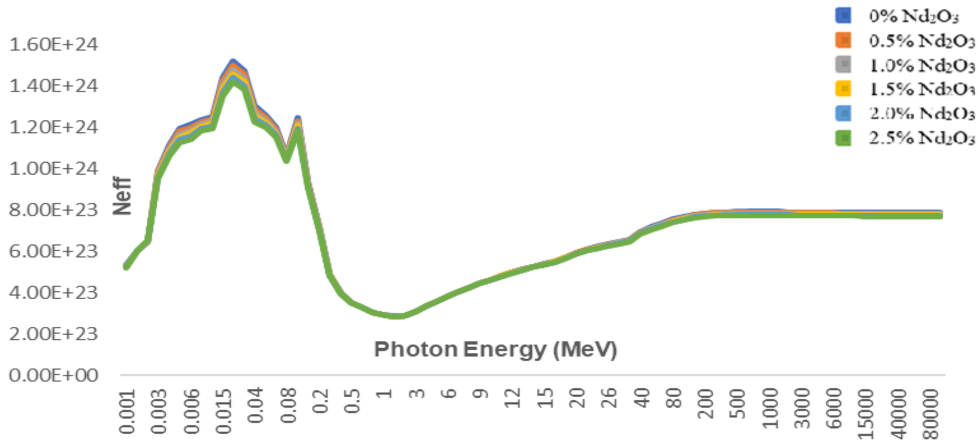


*Fig. 7. $N_{eff}$ of glass samples with different $Nd_2O_3$ concentrations against energy.*

## 4. Conclusion

The results demonstrated a significant improvement in radiation shielding effectiveness with increasing $Nd_2O_3$ content. The glasses doped with higher concentrations of $Nd_2O_3$ exhibited higher LAC and MAC values, while the HVL and MFP decreased, indicating enhanced shielding efficiency. These improvements are related to the high atomic number and density of $Nd_2O_3$, which contribute to greater attenuation of gamma radiation. Overall, the study concludes that $Nd_2O_3$ doped yttrium lead borotellurite glass systems offer promising potential for advanced radiation shielding applications, combining effective gamma-ray attenuation with desirable physical properties.

### Acknowledgments

The author wishes to thank the Ministry of Higher Education (MOHE), Malaysia for the financial support to carry out this research through Fundamental Research Grant Scheme (FRGS) no. 600-IRMI/FRGS 5/3 (039/2019).

## References

[1] S. Jain, J Family Med Prim Care 10(4), 1520 (2021); https://doi.org/10.4103/jfmpc.jfmpc_2292_20

[2] N. A. M. Rusni, H. Laoding, A. Amat, E3S Web of Conferences, EDP Sciences, Jan. (2024); https://doi.org/10.1051/e3sconf/202448103009

[3] M. I. Sayyed, M. A. Abdo, H. E. Ali, H. A. Ahmed, M. S. Sadeq, Optik 278, May (2023); https://doi.org/10.1016/j.ijleo.2023.170738

[4] S. Kaewjaeng, S. Kothan, W. Chaiphaksa, N. Chanthima, R. Rajaramakrishma, H.J. Kim J. Kaewkhao, Radiation Physics and Chemistry, 160, 41-47, Jul. (2019); https://doi.org/10.1016/j.radphyschem.2019.03.018

[5] R. Biswas, H. Sahadath, A. S. Mollah, Md. F. Huq, J Radiat Res Appl Sci, 9(1), 26-34 (2016); https://doi.org/10.1016/j.jrras.2015.08.005

[6] H. O. Tekin, G. ALMisned, Hesham M. H. Zakaly, Abdallah Zamil, Dalia Khoucheich, Ghaida Bilal, Lubna Al-Sammarraie, Shams A. M. Issa, Mohammed Sultan Al-Buriahi, Antoaneta Ene, Open Chem, 20(1), 130-145 (2022); https://doi.org/10.1515/chem-2022-0128

[7] M. Kamislioglu, Results Phys, 22, Mar. (2021); https://doi.org/10.1016/j.rinp.2021.103844

[8] Floressy Juhim, Fuei Pien Chee, Asmahani Awang, Pak Yan Moh, Khairul Anuar Mohd Salleh, Sofian Ibrahim, Jedol Dayou, Amani Alalawi, M.S. Al-Buriahi, Heliyon, 9(11), Nov. (2023); https://doi.org/10.1016/j.heliyon.2023.e22529

[9] M. I. Sayyed, Badriah Albarzan, Aljawhara H. Almuqrin, Ahmed M. El-Khatib, Ashok Kumar, Daria I. Tishkevich, Alex V. Trukhanov, Mohamed Elsafi, Materials, 14(14), Jul. (2021); https://doi.org/10.3390/ma14143772

[10] Y. Azlina, M.N. Azlan, S.S. Hajer, M.K. Halimah, A.B. Suriani, S.A. Umar, R. Hisam, M. H.M. Zaid, S.M. Iskandar, B.K. Kenzhaliyev, A.V. Nitsenko, N.N. Yusof, Boukhris Imed, Opt Mater, 117, Jul. (2021); https://doi.org/10.1016/j.optmat.2021.111138

[11] R. Boodaghi Malidarre, I. Akkurt, Radiation Physics and Chemistry, 212, Nov. (2023); https://doi.org/10.1016/j.radphyschem.2023.111174

[12] C. Devaraja, G. V. Jagadeesha Gowda, K. Keshavamurthy, B. Eraiah, G. Devarajulu, G. Jagannath, Vacuum, 177, 109426 (2020); https://doi.org/10.1016/j.vacuum.2020.109426

[13] E. Sakar, O. F. Ozpolat, B. Alım, M. I. Sayyed, M. Kurudirek, Radiation Physics and Chemistry, 166 Jan. (2020); https://doi.org/10.1016/j.radphyschem.2019.108496

[14] M. R. S. Nasuha, H. Azhan, L. Hasnimulyati, W. A. W. Razali, Y. Norihan, J Non Cryst Solids, 551, Jan. (2021); https://doi.org/10.1016/j.jnoncrysol.2020.120463

[15] ARPANSA, Gamma radiation, Australian Radiation Protection and Nuclear Safety Agency, https://www.arpansa.gov.au/understanding-radiation/what is radiation ionising radiation gamma radiation.

[16] A Acikgoz, Mwaladailah, O L Tashlykov, G Demircan, M Kamislioglu, M M Yas¸Ar, H Ozdogan, N Yorulmaz, Pramana - Journal of Physics, 97(4), Dec. (2023); https://doi.org/10.1007/s12043-023-02629-7

[17] Y. Elmahroug, B. Tellili, C. Souga, Ann Nucl Energy, 75, 268-274 (2015); https://doi.org/10.1016/j.anucene.2014.08.015

[18] M. Kamislioglu, Results Phys, 22, Mar. (2021); https://doi.org/10.1016/j.rinp.2021.103844

[19] H.O. Tekin, Shama A.M. Issa, G. Kilic, Hesham M.H. Zakaly, N. Tarhan, H.A.A. Sidek, K.A. Matori, M.H.M. Zaid, Applied Sciences, 11(3035), (2021); https://doi.org/10.3390/app11073035

[20] O. Kilicoglu, F. Akman, H. Ogul, O. Agar, U. Kara, Radiation Physics and Chemistry, 204, Mar. (2023); https://doi.org/10.1016/j.radphyschem.2022.110676

[21] M. H. A. Mhareb, M. I. Sayyed, T. Flemban, N. Dwaikat, M. G. B. Ashiq, Y. S. M. Alajerami, ISSSD 2020 Online Experimental shielding properties for a novel glassy system, 2020.

[22] M.A.M. Uosif, Shams A.M. Issa, Antoaneta Ene, V. Ivanov, A.M.A. Mostafa, Ali Atta, E.F. El Agammy, Hesham M.H. Zakaly, Journal of Materials Research and Technology, 25, 2088-2096, Jul. (2023); https://doi.org/10.1016/j.jmrt.2023.06.107

[23] Floressy Juhim, Fuei Pien Chee, Asmahani Awang, Pak Yan Moh, Khairul Anuar Mohd Salleh, Sofian Ibrahim, Jedol Dayou, Amani Alalawi, M.S. Al-Buriahi, Heliyon, 9(11), Nov. (2023); https://doi.org/10.1016/j.heliyon.2023.e22529

[24] M.I. Sayyed, Journal of Advanced Research In Applied Sciences And Engineering Technology, 37(2), 156-164 (2024); https://doi.org/10.37934/araset.37.2.156164

[25] E.M. Abou Hussein, Optical and Quantum Electronics, 56, 543 (2024); https://doi.org/10.1007/s11082-023-06180-y

[26] Thair Hussein Khazaalah, Iskandar Shahrin Mustafa, M.I. Sayyed, Azhar Abdul Rahman, Development of Novel Transparent Radiation Shielding, Sustainability, 14(937), (2022); https://doi.org/10.3390/su14020937

[27] Al-Buriahi M.S., C., Eke, S. Alomairy, Journal of Material Science: Materials in Electronics, 32,13906-13916 (2021); https://doi.org/10.1007/s10854-021-05966-8

[28] F. Akman, R. Durak, M. F. Turhan, ad M. R. Kaçal, Applied Radiation and Isotopes, 101, 107-113, (2015); https://doi.org/10.1016/j.apradiso.2015.04.001